molecules

MDPI

Article

Experimental and theoretical approaches of new nematogenic chair architectures of supramolecular H-bonded liquid crystals

O.A. Alhaddad [1], H.A. Ahmed [2,3]*, M. Hagar [2,4]*,

1. College of Sciences, Chemistry Department, Madina Monawara, Taibah University, Saudi Arabia
2. College of Sciences, Chemistry Department, Yanbu, Taibah University, Saudi Arabia., (HA) ahoda@sci.cu.edu.eg, (MH) mohamedhaggar@gmail.com
3. Faculty of Science, Department of Chemistry, Cairo University, Cairo, Egypt.
4. Faculty of Science, Chemistry Department, Alexandria University, Alexandria, Egypt

* Correspondence: H.A. Ahmed, ahoda@sci.cu.edu.eg; M. Hagar , mohamedhaggar@gmail.com.

Received: date; Accepted: date; Published: date

Abstract: New four isomeric chair architectures of 1:1 H-bonded supramolecular complexes were prepared through intermolecular interactions between 4-(2-(pyridin-4-yl)diazenyl-(2-(or 3-)chlorophenyl) 4-alkoxybenzoates and 4-n-alkoxybenzoic acids. The H-bond formation of all complexes was confirmed by differential scanning calorimetry (DSC) and Fourier-transform infrared spectroscopy (FTIR). Mesomorphic characterization was carried by DSC and polarized optical microscopy (POM). It was found that, all prepared laterally choro substituted supramolecular complexes were nematogenic exhibited pure nematic phase and low melting temperature. The thermal stability of the nematic mesophase observed depends upon the location and spatial orientation of the lateral Cl- atom in as well as the length of terminal chains. The density functional theory (DFT) theoretical calculations were discussed to predict the molecular conformation for the formed complexes as well as their thermal parameters. The results of the computational calculations revealed that the H-bonded complexes were in a chair form molecular geometry. Moreover, the results explained the effect the position and orientation of the lateral group as well as the alkoxy chain length on the type and the stability of the nematic mesophase. In addition, their impacts on the estimated thermal parameters of H-bonded complex and how these play an important role in influencing thermal and optical properties.

Keywords: Chair – shaped supramolecular liquid crystals; Hydrogen bonding; Azopyridines; Nematic phase; DFT theoretical calculations; Molecular geometry

1. Introduction

Recently, supramolecular liquid crystals (SMLCs) have an exponentially attraction in attention of scientific researches[1-5]. These systems combine the supramolecular chemistry [6] and liquid crystals [7, 8] with efficient properties for optical and technological potential applications [9]. H-bonding intermolecular interactions are a well-established strategy to design self-assembly LCs through several non-covalent bonds [10-14]. Among the hydrogen bond acceptors and donors, the pair of a carboxylic acid and a pyridine derivative is the best choice in several studies. Moreover, using of multifunctional components in the formation of non-covalent interaction can produce better characteristics supramolecular LC network architectures [6, 7]. Azopyridine molecules are incorporated into liquid-crystal materials to make them photoresponsive [15, 16]due to their ability for *trans-cis*-isomerization upon thermal and photo irradiation. Modifying the core structure or adding lateral substituents to azopyridine-based derivatives can lead to marked changes in photophysical and photochemical properties. [15, 16] An incorporation of lateral groups with different size and polarity widely improves many characteristics of liquid crystalline materials. It could be attributed to the disturbance in the molecular packing that decreases the melting temperature and thermal stability of liquid crystal mesophases. [17-24]. Lately, azopyridines have been used in the formation of nano fiber supramolecular self-assembling and hydrogen/halogen-bonding LCs with photo induced transition phenomena.[25-29]Designing of photosensitive SMLCs through intermolecular interactions using the suitable H-bond donors and acceptors are concerns of our area of interest. [30-36]Anisotropic structures are produced from the overall molecular shape of architectures and the combination of rigid (aromatic) and flexible segments (alkyl chains). Those changes in the characteristics of the LCs may be impact the mesomorphism as well as the properties essential for technical uses. Recently, construction of materials according to computational prediction has a high attention of many researchers [18, 37-46]. Mutual influence of the many optical parameters requires stimulated information about the energies of molecular orbitals as well as the molecular geometries of the LCs. Moreover, density functional theory (DFT) becomes effective popular method for its excellent performance and consistent with the experimental results. [18, 40, 47, 48]

In order to understanding and controlling the mesomorphic properties of the soft material complexes, the goal of present work focus on designing new H-bonded supramolecular architectures of new conformation and discuss the geometrical as well as the thermal parameters of the investigated complexes. Also to study the stability of different spatial oriented lateral polar groups on the thermal and optical behavior of prepared intermolecular H-bonded complexes, which oriented with different angles on the central ring of the Azopyridine-based moiety. Moreover, DFT theoretical calculations will be discussed to predict the molecular conformation for the formed

complexes as well as their thermal parameters. In addition, these calculations will be used to explain the effect the position and orientation of the lateral group as well as the length of the alkoxy chain on the type and the stability of the observed mesophase. Finally, to investigate the impact of the estimated thermal parameters of H-bonded complexes and how these parameters could affect their thermal and optical properties.

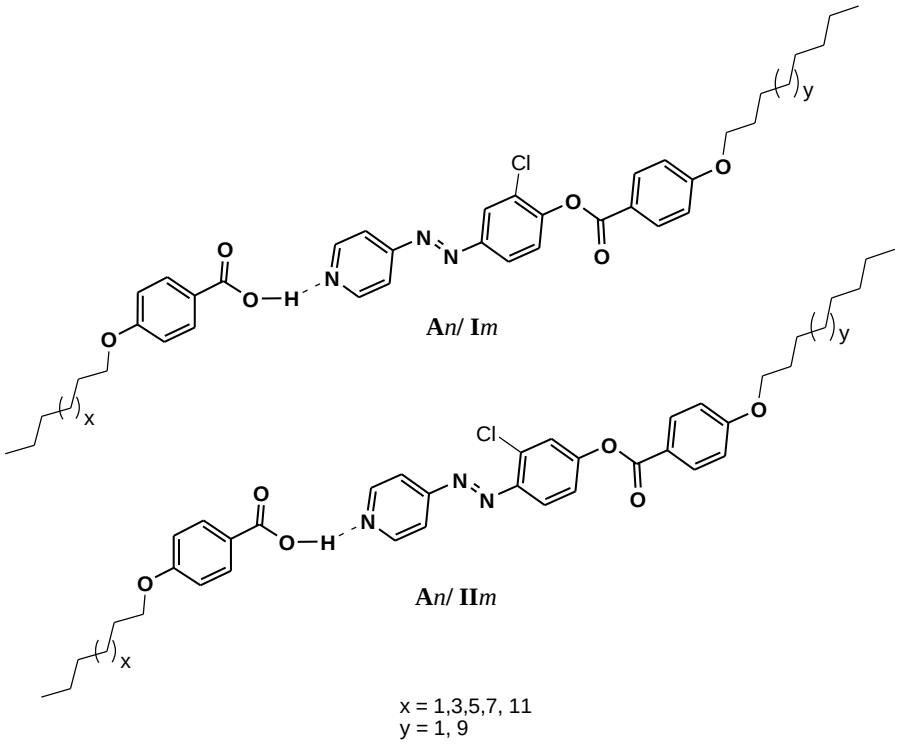

2. Experimental

2.1. Preparation of 1:1 Supramolecular Complexes

4-n-Alkoxy benzoic acids were obtained from Merck (Germany). All the solvents used were of pure grade and purchased from Aldrich (Wisconsin, USA).

4-n-Alkoxy benzoic acids (**A***n*), and lateral chloro pyridine-based derivatives (**I***m* and **II***m*) were checked to exhibit identical transition temperatures as previously reported.[8, 49]

The 1:1 molar ratios of any two complementary components SMHBLCs complexes (**A***n*/**I***m* and **A***n*/**II***m*) were prepared by melting the appropriate amounts of each component, stirring to give an intimate blend and then, cooling with stirring to room temperature (**Scheme 1**). For example to prepare the supramolecular complex **A***10*/**I***8*: 0.0278 mg of 4-decyloxybenzoic acid **A***10* and 0.0466 mg of 4-(2-(pyridin-4-yl)diazenyl-(2-chlorophenyl) 4-octyloxy benzoate **I***8* were melted together to form the complex.

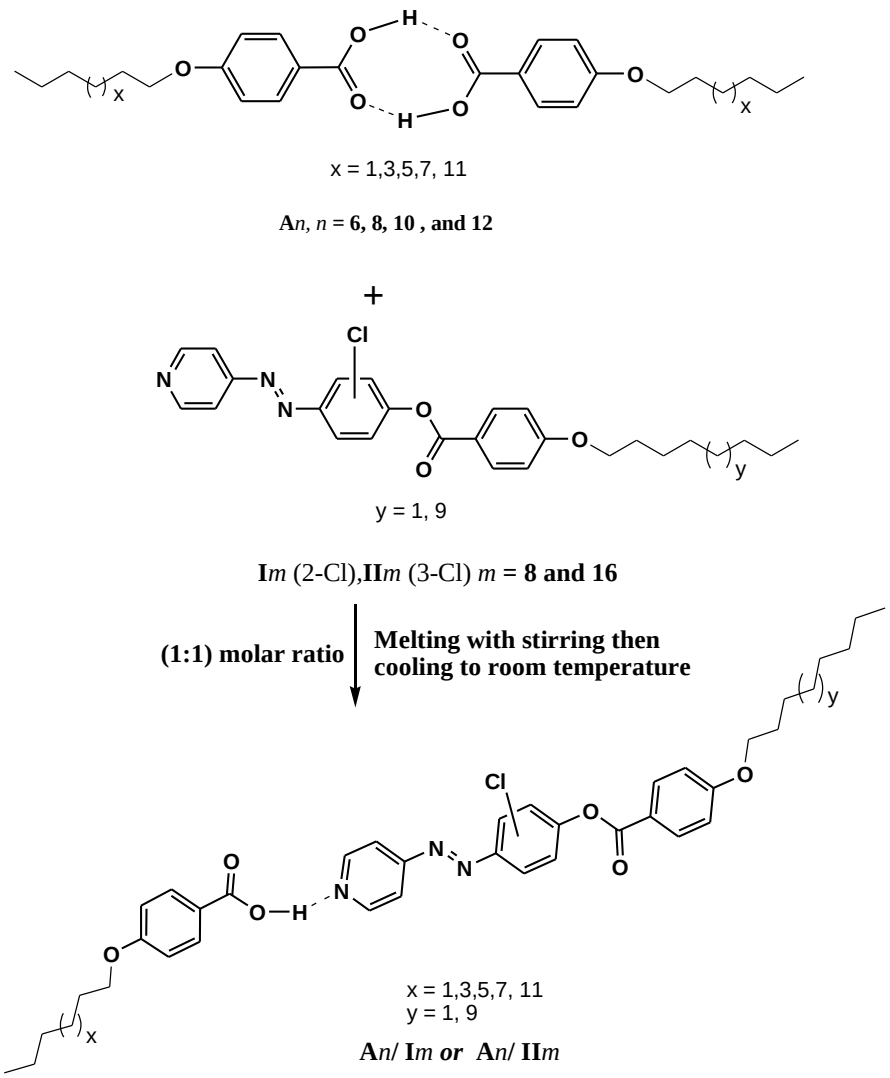

Scheme 1. Preparation of 1:1 SMHB complexes (**A***n*/**I***m* and **A***n*/**II***m*).

2.2. Characterizations

Supramolecular complexes formations were confirmed by TA Instruments Co. Q20 Differential Scanning Calorimeter (DSC; USA), polarized-optical microscopy (POM, Wild, Germany) and FT-IR (Nicolet iS 10 Thermo scientific) spectroscopic analysis.

Calorimetric measurements were carried out using a PL-DSC of Polymer Laboratories, England. The instrument was calibrated for temperature, heat and heat flow according to the method recommended by Cammenga, et. al. [50] Measurements were carried out for small samples (2-3 mg) placed in sealed aluminum pans. All measurements were conducted at a heating rate of 10°C/min in an inert atmosphere of nitrogen gas (10 mL/min). For DSC, the sample was heated from room temperature to 280 °C at heating rate of 10 °C/min under nitrogen atmosphere, and then cooled in the cell to 0 °C. All weighed samples were made using an ultra-microbalance, Mettler Toledo England, with accuracy ±0.0001 gm.

Transition temperatures for the complexes (**A***n*/**I***m* and **A***n*/**II***m*) were investigated by DSC in heating and cooling cycles. The types of the mesophase were identified using a standard polarized-optical microscopy POM (Wild, Germany), attached with Mettler FP82HT hot stage. Measurements were made twice and the results were found to have accuracy in transition temperature and enthalpy within ± 0.2 ^{o}C.

2.3. Computational Methods and calculations

The theoretical calculations for the investigated compounds were carried out by Gaussian 09 software [51]. DFT/B3LYP methods using 6-31G (d,p) basis set was selected for the calculations. The geometries were optimized by minimizing the energies with respect to all geometrical parameters without imposing any molecular symmetry constraints. The structures of the optimized geometries had been drawn with Gauss View [52]. Moreover, the calculated frequencies were carried out using the same level of theory. The frequency calculations showed that all structures were stationary points in the geometry optimization method with none imaginary frequency.

3. Results and Discussion

3.1. FT-IR spectroscopic confirmation of SMHB complexes formation

The formation of the supramolecular complexes has been confirmed by FTIR spectral data. The measurements were performed for the individual components as well as their H-bonded supramolecular complexes. The FTIR spectrum of acids, azopyridine bases and their complexes (**A***12*/**I***16* and **A***12***II***16*as representative examples) are given in **Figure 1**. It has been reported that, no significant effect of the length of the alkoxy chain on the wave number of the C=O group stretching vibration either for the individual acids or the H-bonded complexes [36, 53, 54]. The signal at 1678.2 cm^{-1} was assigned to the stretching vibration of the C=O group of the alkoxy acid, experimentally and theoretically, respectively. The H-bonding between the nitrogen of azopyridines and the carboxylic group of alkoxybenzoic acid of the supramolecular complexes **A***n*/**I***m* and **A***n*/**II***m* replaces the bis H-bonds of the dimeric form of the alkoxybenzoic acid. One of the important evidence of the H-bonded supramolecular complexes formation is the stretching vibration of the C=O carboxylic group either experimentally or theoretically. The sharing of carboxylic group OH-group in H-bonding formation will decreases the strength O-H bond. Theoretically, (**Table 1**), the OH-bond length increased from 0.97588 Å for the free acid to 1.04046 Å and 1.03154 Å for H-bonded complex **A***12*/**I***16* and **A***12*/**II***16*, respectively. Moreover, their wave number of the stretching vibration decreases from 3660.9 cm^{-1}of the free acid to 2508.8 cm^{-1} for isomer **A***12*/**I***16* and 2572.5 cm^{-1} for the other isomer, **A***12*/**II***16*. Similarly, the strength of the C=O bond of the COOH group decreases upon the H-bonding formation, where, the stretching vibration decreases to 1687.0 and 1666.6 cm^{-1} for

H-bonded isomers **A***12*/**I***16*and **A***12*/**II***16* instead of 1691.0 cm^{-1} for the free acid. Obviously, from the theoretical results, the position of the Cl-atom has an intensive effect on the H-bond strength of the H-bonded complex. The presence of the electronegative Cl-atom near the pyridine ring responsible for the H-bond formation for **A***12*/**I***16* complex (the Cl-atom in meta position with respect to the ester group) will disrupt the H-bond formation by decreasing the availability of the lone pair on the N-atom of the pyridine ring. Experimentally, the results of the FT-IR revealed that, no significant effect of the H-bond formation on the C=O group of the free carboxylic acid, only 2 cm^{-1} decreasing, ($\acute{\nu}_{C=O}$ = 1681.7 cm^{-1}). However, the supramolecular complex formation has high stretching vibration effect on the C=O of the ester linkage of the azopyridine base, their wave number increases from 1727.8 to 1743.4 cm^{-1} for complex **A***12*/**I***16*and 15.9 cm^{-1} forthe other complex **A***12*/**II***16*. Moreover, it has been reported [46, 55-60] that, a major evidence on the formation H-bond supramolecular complex is the presence of three vibration bands of Fermi resonance of the H-bonded OH groups **A**-, **B**- and **C**-types. The vibrational peak assigned to **A**-type Fermi band of complex **A***12*/**I***16* and **A***12*/**II***16* presented under the C-H vibrational peaks at 2915 to 2855 cm^{-1}. Moreover, the peak at 2329 (**A***12*/**I***16*) and 2356 cm^{-1} (**A***12*/**II***16*) could be attributed to the O-H in-plane bending vibration as well as its fundamental stretch (**B**-type). However, 1899.3 and 1906.8 cm^{-1} were assigned to **C**-type Fermi band due to the interaction between the overtone of the torsional effect and the fundamental stretching vibration of the OH.

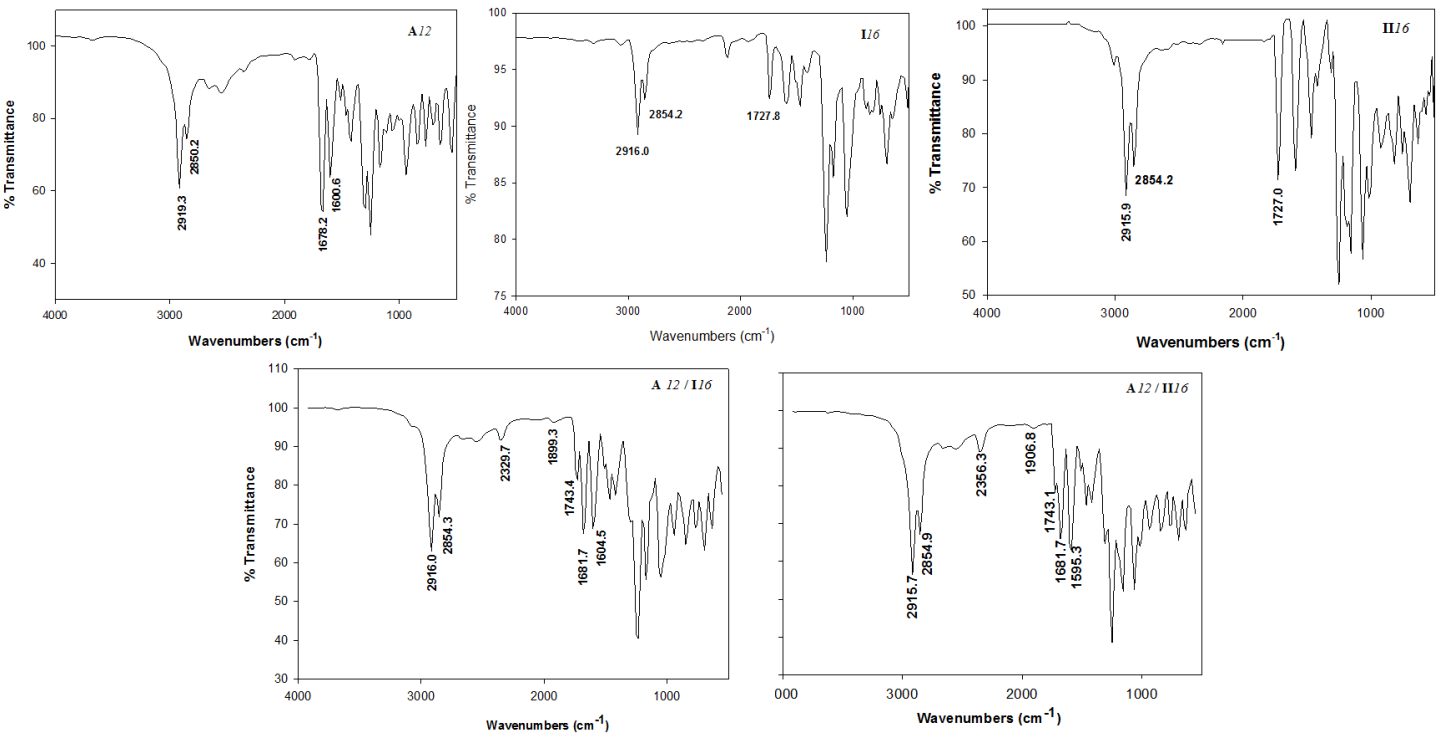

Figure 1. FTIR spectrum of acid **A***12*, azopyridine bases, **I***16*&**II***16*, as well as their 1:1 supramolecular complexes **A***12*/**I***16* and **A***12***II***16***.**

Table 1. The calculated bond length (Å) wave numbers (cm^{-1}) of characteristic groups of **A***12*, **I***16*, **II***16*, **A***12*/**I***16*and**A***12*/**II***16*.

Compound	υ_{OH} (cm^{-1})	O-H (Å)	$\upsilon_{C=O}$ (cm^{-1})	C=O (Å)	$\upsilon_{C=NPyr}$ (cm^{-1})	C=N_{Pyr} (Å)	υ_{H-bond} (cm^{-1})	H-bond (Å)
A*1* ٢	3660.9	0.97588	1691.0	1.23711				
I*16*					1595.0	1.35596		
II*16*					1593.5	1.35100		
A*1* ٢/**I***16*	2511.٤	1.04033	1686.٨	1.25486	1609.2	1.35377	2511.٤	1.60554
A*1* ٢/**II***16*	2573,٠	1.03151	1666.6	1.25194	1599,٤	1.35243	2573,٠	1.61965

3.2. Mesomorphic and optical behavior

All 1:1 molar ratio complexes, **A***n*/**I***m* and **A***n*/**II***m*, were made from each of the two homologues of the azopyridine base (**I***m*and **II***m*) and each of the four homologues of the acid, **A***n*. The prepared complexes were characterized for their mesomorphic properties by DSC and POM. The textures observed by POM were verified by the DSC measurements and types of mesophases were identified for all prepared supramolecular complexes **A***n*/**I***m* and **A***n*/**II***m*. DSC thermograms of the 1:1 supramolecular complexes **A***12*/**I***16* and **A***12*/**II***16*, as examples, are depicted in **Figures S1** and **S2** (see supplementary data). Similarly, DSC behaviors were observed when the prepared mixtures were subjected to repeat heating/ cooling cycles this meaning that our present work displays a pronounced thermal stability.

Transition temperatures and their associated enthalpies of transition values were measured by DSC for all prepared complexes and are summarized in **Table 2.** The effect of terminal alkoxy chain length of the acid component (*n*) represented graphically, as function of *m* of the two isomeric groups of base moieties (**I***m* and**II***m*) in **Figures 2** and **3**, respectively. The results of **Table 2** and **Figures 2** and **3** showed that, independently of neither of acid or base terminal alkoxy chains (*n* and *m*), the nematic (N) mesophases are observed for all prepared lateral Cl complexes. In most cases, the N phase stability (T_{N-I}) was found to decrease with the increment of *n*. As shown from **Figure 2**, the complexes **A***n*/**I***8*exhibit an enantiotropic nematic phase and the nematic enhancement is slightly increases with the increase of *n* (**Figure 2a**). While, the longer base terminal (*m* =16, **Figure 2b**),the prepared complexes **A***n*/**I***16*showed a stable nematic phase upon heating and cooling except **A***12*/**I***16*exhibits monotropic N phase behavior. Upon heating, **A***12*/**I***16* converts to isotropic liquid at 80.5 °C without showing any LC phase, whereas, in the cooling scan it exhibits a nematic mesophase start from 71.5 °C.

Figure 3 shows the mesomorphic behavior of base moiety **II***m* (the lateral Cl group introduced at the meta-position with respect to the ester carbonyl core) with variable alkoxy chains. It could be seen from **Figure 3a**, the supramolecular complexes **A***n*/**II***8* exhibit different nematic behavior than

the corresponding isomeric complexes **A***n*/**I***8*, whereas, **A***n*/**II***8* have relatively wide enantiotropic nematic ranges with higher value for the complex **A***6*/**II***8* (~ 36.4 °C) and the wide nematic rang value for **A***12*/**II***8*monotropically. Moreover, the nematic stability decreases with the alkoxy chain length (*n*) of the acid component. In addition, the supramolecular complexes melting temperatures are slightly affected by the length of the alkoxy chain of the acid. Finally, it is obvious from **Figure 3b** (**A***n*/**II***16*) that, an independent effect of the alkoxy chain length of the acid on a monotropic nematic phase covered all supramolecular complexes. From the present investigation, it would be expected that, the increment in the molecular anisotropy due to the orientation of the lateral electron-withdrawing Cl atom in the supramolecular geometry impacted the stability of nematic phase that agrees with our previous work [31, 61].

Furthermore, the addition of lateral Cl atom in supramolecular architectures weakens the side by side cohesion interactions thus enhances a nematic phase for all 1:1 complexes. In addition, the molecular geometry and size of the lateral substituent impact the mesophase stability and the polarizability of whole molecule [19, 20, 62]. It found that the length of the alkoxy chain, the polarity as well as the position (or orientation) of the lateral group are importance factors in determining the types and the range of the stability of the mesophase. Images of the mesophase as representative examples from POM are shown in **Figure 4**. Schlieren texture of nematic phase was observed for all complex prepared.

Table 2: Phase transition temperatures (°C), enthalpy of transitions (kJ/mol) and normalized entropy change for the supramolecular complexes **A***n*/**I***m* and **A***n*/**II***m*.

System	T_{Cr-N}	ΔH_{Cr-N}	T_{N-I}	ΔH_{N-I}	$\Delta S/R_{N-I}$
A*6*/**I***8*	60.1	71.75	77.3	1.66	2.58
A*8*/**I***8*	61.9	61.59	75.8	1.56	2.48
A*10*/**I***8*	66.2	79.71	80.0	2.45	3.68
A*12*/**I***8*	68.2	68.49	80.1	2.32	3.48
A*6*/**I***16*	74.4	87.51	89.8	2.32	3.11
A*8*/**I***16*	73.7	89.04	87.1	1.96	2.71
A*10*/**I***16*	77.8	87.68	86.3	3.36	4.68
A*12*/**I***16*	80.5	98.32	71.5*	2.76	4.64
A*6*/**II***8*	77.9	83.41	114.3	2.85	3.00

A*8*/**II***8*	77.3	80.56	87.4	1.96	2.70
A*10*/**II***8*	81.8	84.80	79.5*	2.08	3.15
A*12*/**II***8*	84.9	86.50	50.1*	2.97	7.13
A*6*/**II***16*	88.1	92.56	82.9*	3.16	4.58
A*8*/**II***16*	90.1	94.13	82.5*	2.60	3.79
A*10*/**II***16*	92.2	96.16	79.0*	3.50	5.33
A*12*/**II***16*	93.3	96.34	80.4*	3.63	5.43

Abbreviations: $T_{Cr\text{-}N}$ = crystal to nematic phase transition; $T_{N\text{-}I}$ = Nematic to isotropic liquid transition. $\Delta H_{Cr\text{-}N}$= crystal to nematic phase transition; $\Delta H_{N\text{-}I}$= Nematic to isotropic liquid transition; $\Delta S/R_{N\text{-}I}$ normalized entropy transition of nematic to isotropic liquid.

*Monotropic transition

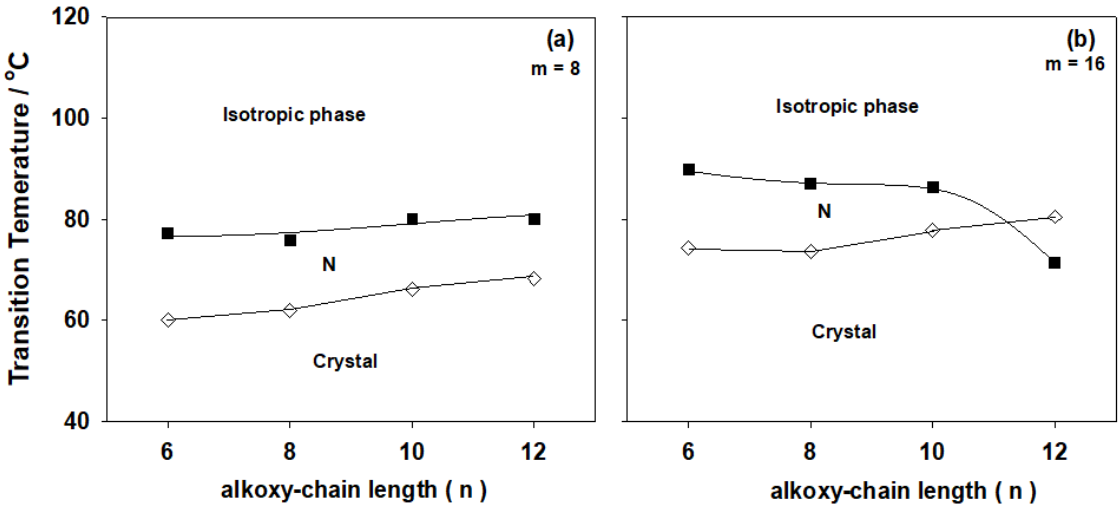

Figure 2. Dependence of the alkoxy-chain length of the acid component (*n*) of the lateral Cl azopyridines (**I***m*) on the mesophase behavior of the 1:1 supramolecular hydrogen-bonded complexes (**a**) *m* = 8; (**b**) *m* = 16. .

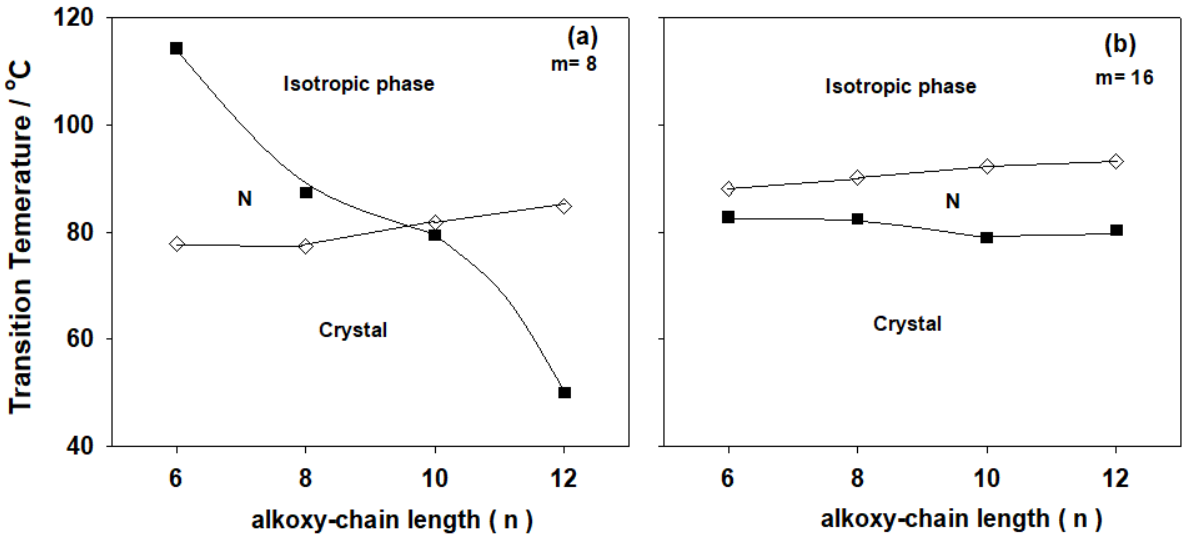

Figure 3. Dependence of the alkoxy-chain length of the acid component (*n*) of the lateral Cl azopyridines (**II***m*) on the mesophase behavior of the 1:1 supramolecular hydrogen-bonded complexes (**a**) *m* = 8; (**b**) *m* = 16.

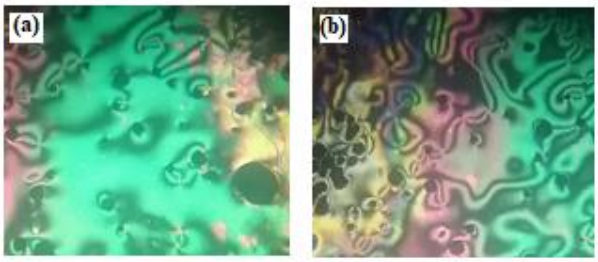

Figure 4. Nematic phase textures under POM of the supramolecular complexes (a) **A***10*/**I***8* at 72.0 °C upon heating; and (b) **A***12*/**II***16* at 77.0 °C upon cooling.

3.2.Effect of polarity and orientation of lateral substituent on the supramolecular hydrogen- bonded complexes stability

In order to study the effect of polarity and position (spatial orientation) of the lateral group on the mesophase thermal stability (**T**c) of 1:1 supramolecular hydrogen-bonded complexes, a comparison was constructed between mesophase stabilities (***T***c) of present lateral Cl complexes (**A***n*/**I***m* and **A***n*/**II***m*) and their corresponding lateral CH_3 supramolecular H-bonded complexes (**A***n*/**III***m* and **A***n*/**IV***m*) [8, 63], as well as the laterally neat (**A***n*/**V***m*) [33]. All data were represented graphically in **Figure 5a-d**. It had been found that, the location and the inductive effect of the lateral substituent incorporated in base complement impacts the polarizability between H-donors and H-acceptor and thus affects the strength of the hydrogen bond [55]. However, the polarity of both components was not affected by the length of the terminal alkoxy chain **(Figure 5a-d)**. Also, the laterally neat supramolecular H-bonded complexes (**A***n*/**V***m*) have the highest thermal stability with

respect to the derivatives of electron donating CH_3 and electron withdrawing Cl lateral substituents. In addition, the nematic mesophase in the present investigation (lateral Cl complexes, **A***n*/**I***m* and **A***n*/**II***m*) is observed instead of the smectic C of the lateral CH_3 and neat supramolecular complexes. Thus the nature of intermolecular interactions between molecules affects the stability as well as the type of the mesophase. The lateral electron withdrawing Cl-atom of the complexes **A***n*/**I***m* and **A***n*/**II***m* predominates the end to end interaction to enhance a less ordered phase (nematic), while the strong backing side by side interactions in case of lateral CH_3 (**A***n*/**III***m* and **A***n*/**IV***m*)and laterally neat (**A***n*/**V***m*) complexes to observe more ordered mesophase (SmC).

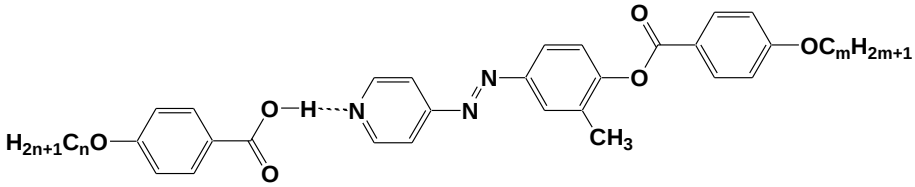

A*n*/**III***m*

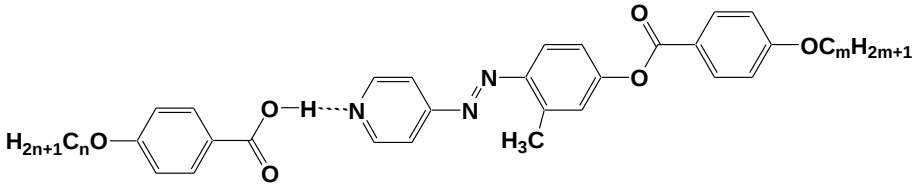

A*n*/**IV***m*

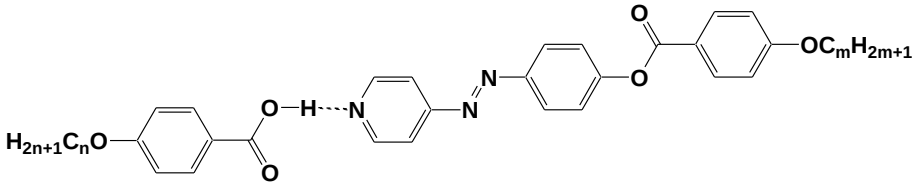

A*n*/**V***m*

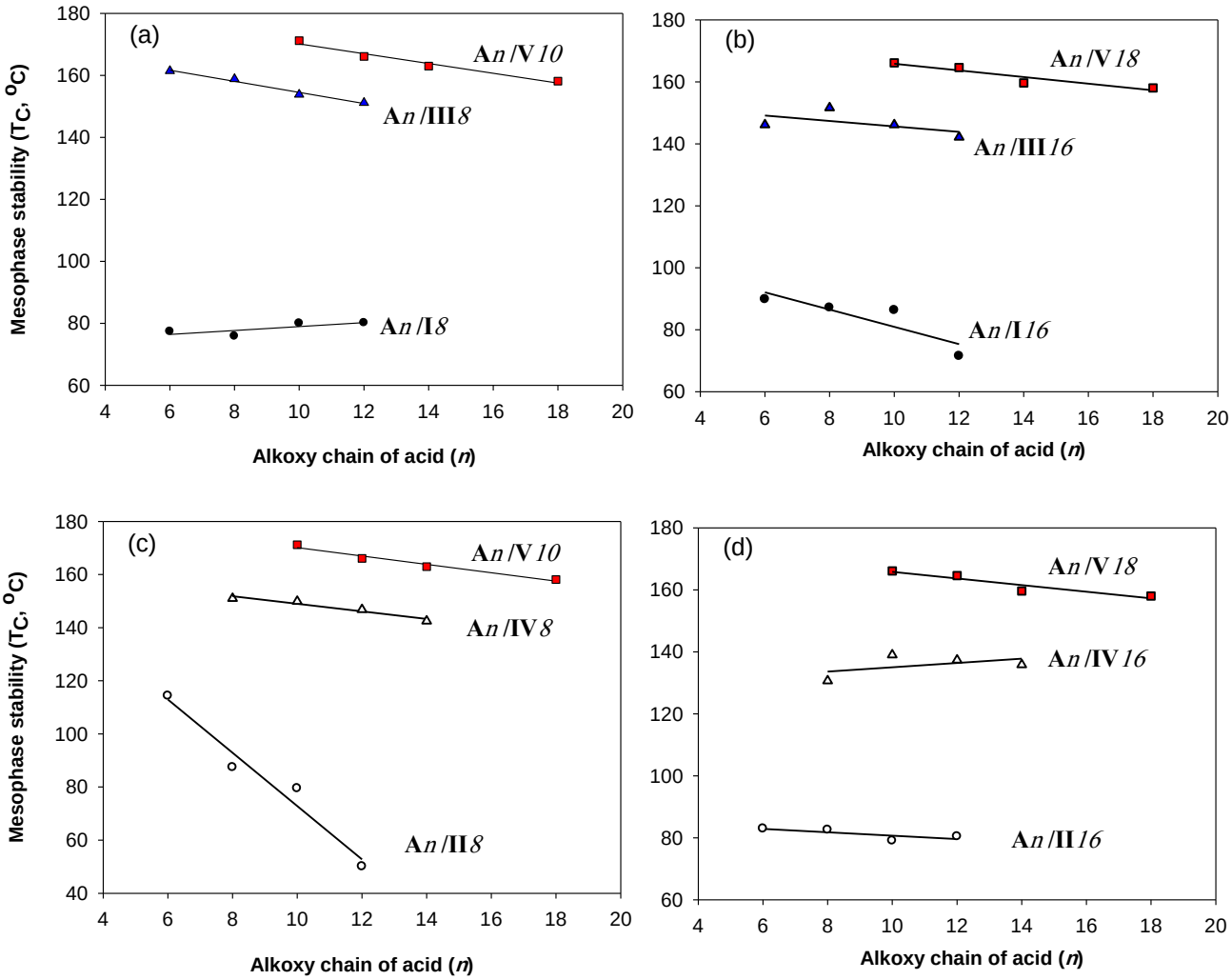

Figure 5. Mesophase stability temperature (*T*c) dependency on the terminal alkoxy chain length (*n*) of the acid complement; **A***n*/**I***m* (●); **A***n*/**II***m* (○); **A***n*/**III***m* (▲); **A***n*/**IV***m* (Δ); **A***n*/**IV***m* (■).

3.3. DFT calculations

3.3.1. Relationship between experimental and theoretical parameters

The theoretical DFT calculations were performed in gas phase by DFT/B3LYP method at 6-31G (d,p) basis set. All optimum compounds are stable and this is approved in the term of the absence of the imaginary frequency. The results of the theoretical DFT calculations for lateral complexes of ortho chloro derivatives with respect to the ester group (**A***n*/**I***m*)as well as the otherisomeric supramolecular complex (meta chloro with respect to the ester group) **A***12*/ **II***16*and **A***16*/ **II***16*showed a chair geometry for all investigated compounds. The three phenyl rings (two of the

azopyridine base and one of the 4-alkoxybenzoic acid) of the H-bonded complexes are completely planar for both supramolecular H-bonded complexes. Recently, our group reported that [36], the chair forms conformation do not permit a strong lateral interaction leaving the end to end aggregation of the chains to be the predominant interaction. The pronounced terminal interaction could be a good explanation for the enhancement of the nematic mesophases observed for all alkoxy chain lengths of the H-bonded complexes over the parallel interaction that enhances the smectic phase formation, **Figure 6**.The estimated DFT calculations for thermal parameters, dipole moment and the polarizability of the prepared supramolecular hydrogen bonding liquid crystal complexes **A***12*/ **I***16*and **A***n*/**II***m* are summarized in **Table 3**.

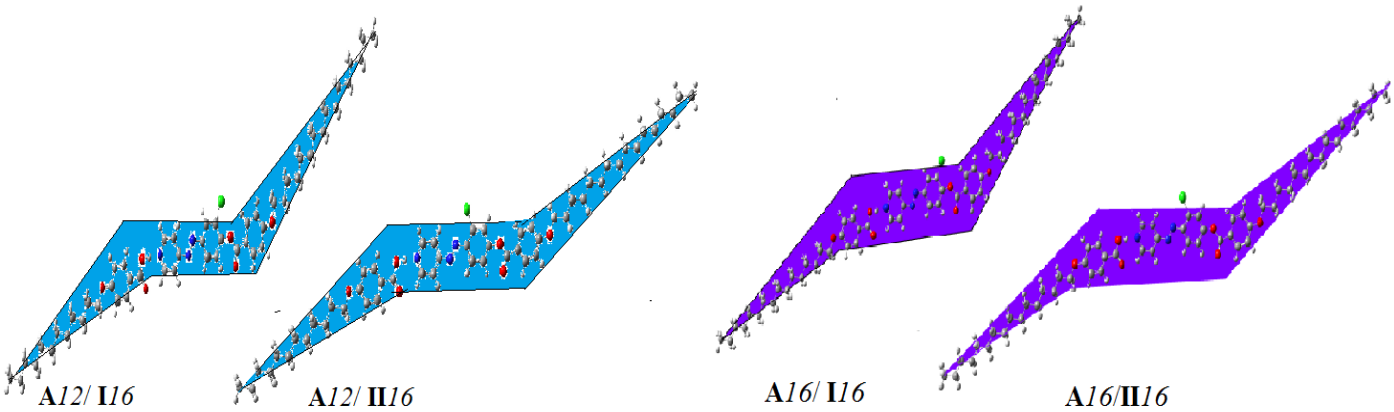

Figure 6. Optimized chair geometrical structures of **A***12*/ **I***16*, **A***12*/**II***16*, **A***16*/ **I***16*, and **A***16*/**II***16*.

Table 3.Thermal parameters (Hartree/Particle) and Dipole Moment (Debye) of **A***12*/ **I***16*, **A***16*/ **I***16* and **A***n*/**II***m*.

Parameter	A1 ٢/ I16	A16/ I16	A6/ II16	A8/ II16	A10/ II16	A12/ II16	A16/ II16
E_{corr}	1.186685	1.300871	1.023466	1.081011	1.138569	1.196254	1.311264
ZPVE	-3138.763063	-3295.897217	-2902.467359	-2981.017950	-3059.568525	-3138.119038	-3295.220301
E_{tot}	-3138.693654	-3295.822383	-2902.406598	-2980.954492	-3059.502386	-3138.050272	-3295.146120
H	-3138.692710	-3295.821439	-2902.405653	-2980.953548	-3059.501442	-3138.049327	-3295.145176
G	-3138.893164	-3296.035253	-2902.583960	-2981.137997	-3059.692422	-3138.245921	-3295.355528
Total Dipole	6.8397	6.8408	8.8893	8.8808	8.8646	8.8632	8.8598
Polarizability α	741.05	788.27	638.07	660.73	683.18	705.30	749.78

ZPVE: Sum of electronic and zero-point energies; E_{tot}: Sum of electronic and thermal energies; H: Sum of electronic and thermal

As shown from **Table 3** and **Figure 6**,the length the alkoxy chain of the homologues series enhancement the calculated thermal energy. As the chain length increases more packing of the molecules is permitted and consequently, the stability of the molecules increases[36, 47, 49, 53, 64-66]. Obviously, there is no significant effect of the alkoxy chain length on the dipole moment. However, the position and the spatial orientation of the Cl-atom has high impact on the magnitude of the dipole moment, 6.8408 and 8.8598 Debye for ortho (**A**12/ **I***16*) and meta (**A**12/ **II***16*) chloro with respect to the carboxylate linkage, respectively. On the other hand, **Figure 7** illustrates the

relationship between the alkoxy chain length of acid moiety (*n*) and the polarizability. As the chain length increases the polarizability increases, and so, the candidate of the highest chain length showed the maximum polarizability and could be predicted to have the best characteristics in NLO applications. Moreover, the position and the orientation of the chloro atom affects the predicted stability as well as the polarizability, the ortho chloro derivative with respect to the ester group (**A***n*/ **I***m*) showed higher polarizability and lower stability rather than that of the other isomer (**A***n*/ **II***m*), the difference was 38.4 Bohr^3 and 424.36 Kcal/mole, respectively, for *n=12* ,*m* =16. The higher stability of the ortho chloro derivatives could be illustrated in the term of its high degree of interaction of the molecules which permits more packing of the compounds rather than that of the meta derivatives.

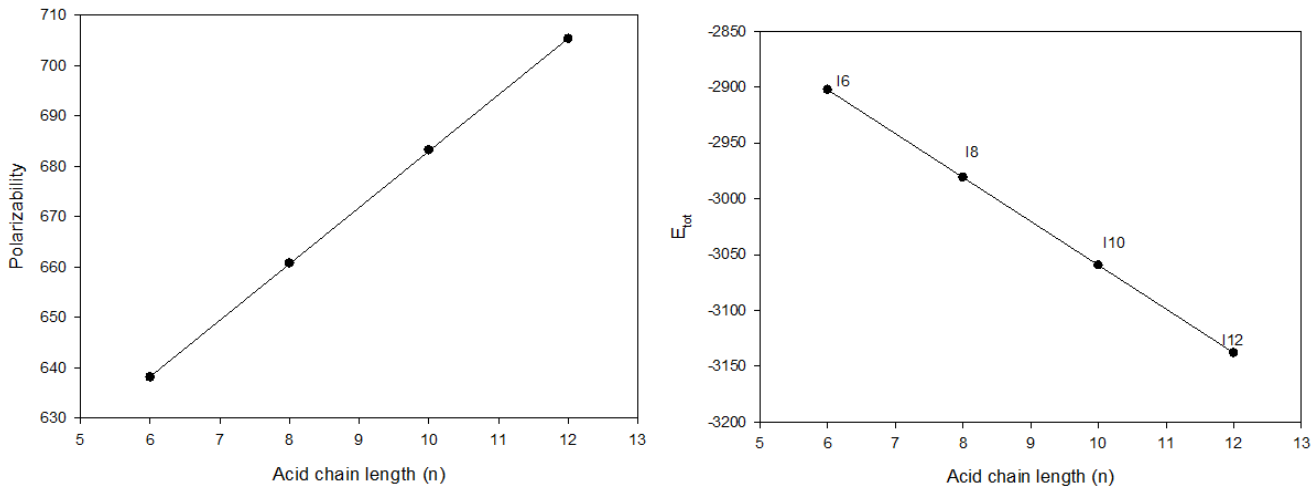

Figure 7. Dependence of the acid akoxy chain-length of SMHB complexes **A***n*/ **II***m* on the (a) the calculated polarizability and (b) thermal energies.

Figure 8 shows the relationship between the length of the acid alkoxy groups and the mesophase nematic stability of 1:1 mixtures **A***n*/ **I***m* against the calculated thermal energy (**E**$_{tot}$) and the polarizability (α). As shown from the figure, the length terminal alkoxy chain has high effect on the mesophases stability of the nematic phase. The calculated thermal energy decreases with the length of the chain and mesophase stability decreases, the similar behaviour was noticed with polarizability. The mesophase stability gradually decreases with the chain length up to *n*=10 then sharp decrements were observed either with the estimated energy or polarizability. This result could be attributed to the high degree of the terminal aggregation at shorter chain lengths rather than that of the longer one which permits more parallel. The chair conformer structure of the H-bonded supramolecular compounds under investigation could permits the maximum end to end interaction for shorter chain lengths while for the longer one this interaction could be decreased with enhancement of side-side aggregation of alkoxy chains and the ester carbonyl moieties, that decreases the mesophase stability of the formed mesophase.

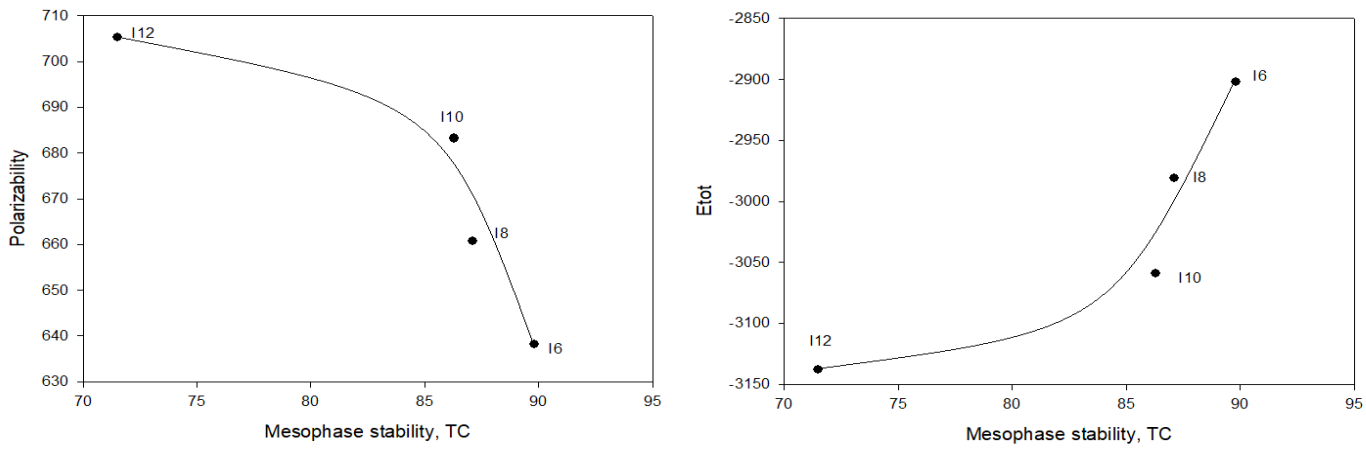

Figure 8. The relationship of the akoxy chain-length / mesophase stability of 1:1 complexes **A***n*/ **II***16* against (a) the calculated polarizability and (b) the total predicted E_{tot}.

3.3.2.Entropy change of SMHB complexes

Terminal alkoxy chains have pronounce role as they are flexible and can easily make multi-conformational changes. An enhancement of the entropy change is observed in all supramolecular H-bonded complexes due to the increment in the conformational and orientation changes of the whole complex. A comparison of the normalized entropy changes for SMHB complexes **A***n*/**I***16*, **A***n*/**II***16*, **A***n*/**III***16*, and **A***n*/**IV***16* was depicted in **Figure 9**. Entropy of transitions (*ΔS*/R) was constructed graphically as a function of the terminal alkoxy-chain length of acid component (*n)* for different lateral substituted supramolecular complexes. **Figure 9** shows that, independent on the terminal flexible chains, an irregular entropy change was observed. That irregular change may be explained to the intermolecular interactions due to the location and rotation as well as the polarity of lateral substituent affect on the ordering of whole complex.[67, 68] The high dipole moment of **A***n*/**II***16* than **A***n*/**I***16* is accompanied by more conformational entropy changes due to good packing of lateral meta Cl supramolecular complexes molecules than the ortho Cl isomers. In contrast for the lateral electron donating CH_3 group, lower entropy transitions observed for meta CH_3 SMHB complexes than the ortho CH_3 isomeric complexes. These results could be explained in terms of the high degree of alignment of the molecules in case of electron donating lateral substituent (CH_3) in the smectic mesophase that highly decreases the entropy with respect to the less ordered nematic mesophase in case of lateral electron withdrawing group (Cl). The large value of entropy in many cases may be explained by the intermolecular interactions due to the location and rotation as well as the polarity of the lateral Cl-atom which enhancement the ordering of whole supramolecular complex. Moreover, non-correlation between the entropies and the terminal alkoxy-chain length may be due to the irregular change of lateral adhesion upon the increase of the total molecular length.

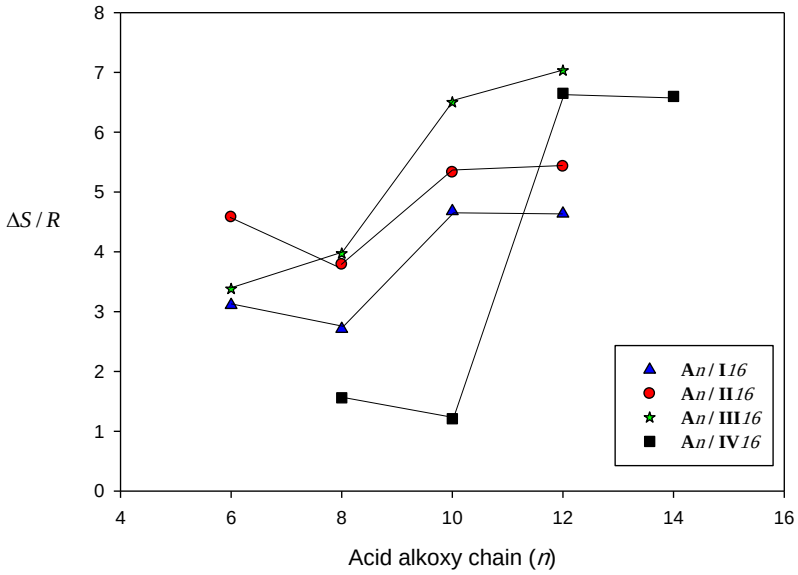

Figure 9. Comparison of the entropy changes of nematic transitions for SMHB complexes **A***n*/**I***16* (▲); **A***n*/**II***16* (●); **A***n*/**III***16* (*); **A***n*/**IV***16* (■).

3.3.3. Frontier molecular orbitals and molecular electrostatic potential

Figure 10 summarizes the predicted ground state isodensity surface plots for the FMOs HOMO (highest occupied molecular orbital) and LUMO (lowest unoccupied molecular orbital)) as well as their energies difference (**ΔE**) of the compounds under investigation **A***n*/**II***m* and **A***12*/**I***16* as examples. As shown from **Table 4**,FMO energy gap and the global softness (**S**) were not significantly affected by the length of the terminal alkoxy chain of compounds **A***n*/**II***m*. However, the position and the orientation of the lateral Cl atom have high impact on the energy difference between the FMOs. The attachment of the Cl atom at the ortho position with respect to the ester linkage increases the energy difference between FMOs (HOMO and LUMO) than that at the meta position. This result could be help in building of the molecules in a certain isomerism (positional and/or orientational) that would improve their characteristics to offer proper applications.

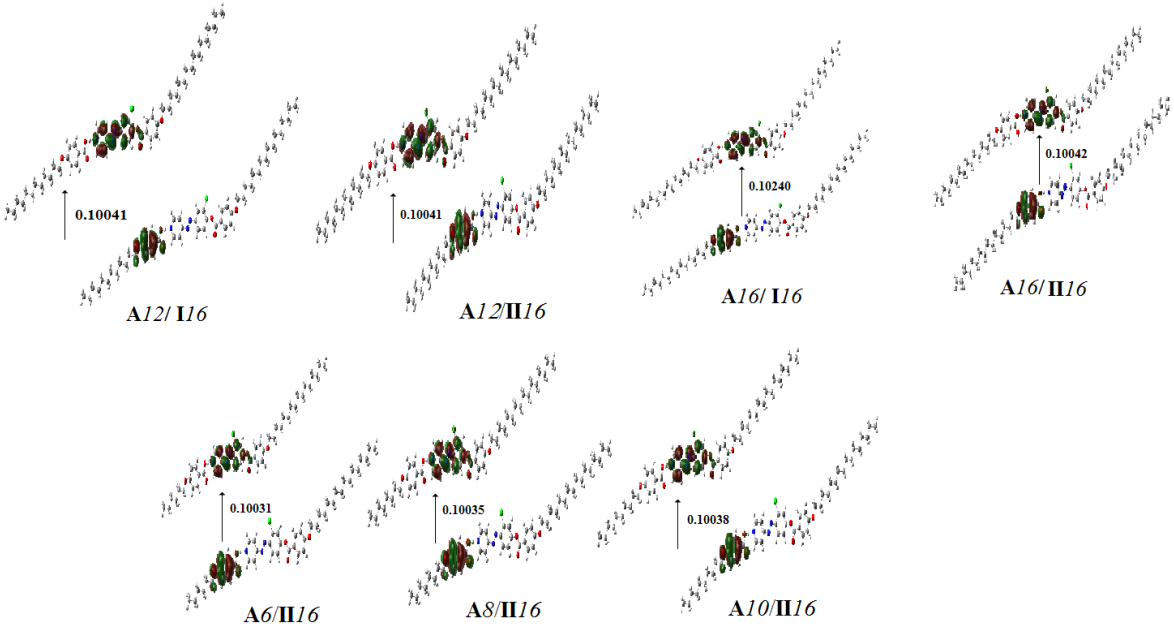

Figure 10. The calculated ground state isodensity surface plots for frontier molecular orbitals of **A***12*/ **I***16* **,** **A***16*/ **I***16*and **A***n*/**II***m.*

Table 4. Molecular orbital energies and global softness (**S**) of **A***12*/ **I***16***,** **A***16*/ **I***16*and **A***n*/**II***m.*

Compound	E_{HOMO} (a.u)	E_{LUMO} (a.u)	ΔE(E_{LUMO}-E_{HOMO}) (a.u)	S= 1/ ΔE
A*1* ٢/**I***16*	-0.21486	-0.11445	0.10041	9.959167
A*16*/**I***16*	-0.22511	-0.12271	0.10240	9.765625
A*6*/**II***16*	-0.21484	-0.11453	0.10031	9.969096
A*8*/**II***16*	-0.21484	-0.11449	0.10035	9.965122
A*10*/**II***16*	-0.21484	-0.11446	0.10038	9.962144
A*12*/**II***16*	-0.21486	-0.11445	0.10041	9.959167
A*16*/**II***16*	-0.21486	-0.11444	0.10042	9.958176

The charge distribution map for the complexes **A***12*/ **I***16*, **A***16*/ **I***16*and **A***n*/**II***m* was calculated under the same basis sets according to molecular electrostatic potential (MEP) (**Figure 11**). The red region (negatively charged atomic sites) was distributed on the aromatic moiety and the maximum was carbonyl oxygen of the H-bonded carboxylic group, while alkoxy chains showed the least negatively charged atomic sites (blue regions). As shown from **Figure 11,** there is no significant effect of either the location, the orientation of Cl atom or the alkoxy-chain length on the charge distribution. This could explain the reason of alteration of the type of the mesophase of the compounds under investigation in the term of the competitive interaction between end-to-end and side-side interaction by increasing of the chain length rather than the change of the charge distribution.

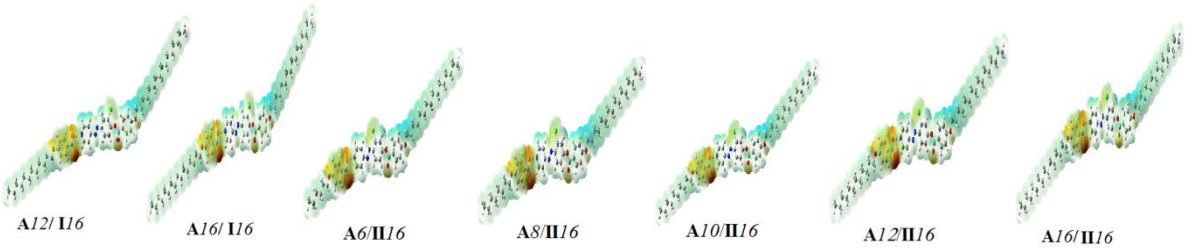

Figure 11. Molecular Electrostatic potentials (MEP) of **A***12*/ **I***16* **,** **A***16*/ **I***16*and **A***n*/**II***m*.

4. Conclusion

Four new isomeric series of 1:1 SMHB complexes in chair-shaped liquid crystalline were constructed based on laterally Cl azopyridine derivatives and 4-alkoxybenzoic acids. All investigated complexes were confirmed by DSC, POM and FT-IR Fermi bands. It was found that all present 1:1 mixtures are purely nematogenic with low melting temperatures. The experimental and DFT theoretical calculations results revealed that the H-bonded complexes were in a chair form molecular geometry. Moreover, the results of the DFT show that the position and orientation of the lateral group as well as the alkoxy chain length affects the type and the stability of the nematic mesophase. The position and the spatial orientation of the Cl-atom has high impact on the magnitude of the dipole moment as well as the polarizability. FMO energy gap and the global softness (**S**) were not significantly affected by the length of the terminal alkoxy chain of compounds. However, the position of the lateral Cl atom has high impact on the energy difference between the FMOs. The higher stability of the ortho chloro derivatives was illustrated in the term of its high degree of interaction of the molecules which permits more packing of the compounds rather than that of the meta derivatives. It could be concluded that, the designing of new nematogenic supramolecular H- bonded conformers with certain molecular geometry offer a new phase transition phenomena that could be promising for proper optical applications. In addition, alteration of thermal and optical parameters by H-bonded complex formations and showing how could play an important role in improving the optical properties.

Conflicts of Interest

"The authors declare no conflict of interest"

References

[1] P. Shen, X. Zhang, H. Lu, Z. Su, Y. Zhou, B. Song, X. Li, X. Yang, Y. Tu, C.Y. Li, Effect of Fullerene Volume Fraction on Two-Dimensional Crystal-Constructed Supramolecular Liquid Crystals, Chemistry–An Asian Journal 14(1) (2019) 125-129.

[2] M. Lehmann, M. Dechant, L. Gerbig, M. Baumann, Supramolecular click procedures in liquid crystals, Liquid Crystals (2019) 1-10.

[3] M. Saccone, M. Pfletscher, S. Kather, C. Wölper, C. Daniliuc, M. Mezger, M. Giese, Improving the mesomorphic behaviour of supramolecular liquid crystals by resonance-assisted hydrogen bonding, Journal of Materials Chemistry C (2019).

[4] V.S. Sharma, A.P. Shah, A.S. Sharma, A new class of supramolecular liquid crystals derived from azo calix [4] arene functionalized 1, 3, 4-thiadiazole derivatives, New Journal of Chemistry 43(8) (2019) 3556-3564.

[5] X. Wang, L. Bai, S. Kong, Y. Song, F. Meng, Star-shaped supramolecular ionic liquid crystals based on pyridinium salts, Liquid Crystals 46(4) (2019) 512-522.

[6] H. Kihara, T. Kato, T. Uryu, J.M. Frechet, Supramolecular liquid-crystalline networks built by self-assembly of multifunctional hydrogen-bonding molecules, Chemistry of materials 8(4) (1996) 961-968.

[7] H. Kihara, T. Kato, T. Uryu, J.M. Frechet, Induction of a cholesteric phase via self-assembly in supramolecular networks built of non-mesomorphic molecular components, Liquid crystals 24(3) (1998) 413-418.

[8] M.M. Naoum, A.A. Fahmi, S.Z. Mohammady, A.H. Abaza, Effect of lateral substitution on supramolecular liquid crystal associates induced by hydrogen-bonding interactions between 4-(4′-pyridylazo-3-methylphenyl)-4″-alkoxy benzoates and 4-substituted benzoic acids, Liquid Crystals 37(4) (2010) 475-486.

[9] A. Gowda, L. Jacob, N. Joy, R. Philip, R. Pratibha, S. Kumar, Thermal and nonlinear optical studies of newly synthesized EDOT based bent-core and hockey-stick like liquid crystals, New Journal of Chemistry 42(3) (2018) 2047-2057.

[10] G.W. Gray, B. Jones, The mesomorphic transition points of the para-normal-alkoxybenzoic acids-a correction, ROYAL SOC CHEMISTRY THOMAS GRAHAM HOUSE, SCIENCE PARK, MILTON RD, CAMBRIDGE …, 1953, pp. 4179-4180.

[11] T. Kato, J.M. Frechet, A new approach to mesophase stabilization through hydrogen bonding molecular interactions in binary mixtures, Journal of the American Chemical Society 111(22) (1989) 8533-8534.

[12] T. Kato, P.G. Wilson, A. Fujishima, J.M. Fréchet, Hydrogen-bonded liquid crystals. A novel mesogen incorporating nonmesogenic 4, 4′-bipyridine through selective recognition between hydrogen bonding donor and acceptor, Chemistry letters 19(11) (1990) 2003-2006.

[13] T. Kato, J.M. Frechet, P.G. Wilson, T. Saito, T. Uryu, A. Fujishima, C. Jin, F. Kaneuchi, Hydrogen-bonded liquid crystals. Novel mesogens incorporating nonmesogenic bipyridyl compounds through complexation between hydrogen-bond donor and acceptor moieties, Chemistry of materials 5(8) (1993) 1094-1100.

[14] T. Kato, J.M. Fréchet, Hydrogen bonding and the self-assembly of supramolecular liquid-crystalline materials, Macromolecular Symposia, Wiley Online Library, 1995, pp. 311-326.

[15] Y. Chen, H. Yu, M. Quan, L. Zhang, H. Yang, Y. Lu, Photothermal effect of azopyridine compounds and their applications, RSC Advances 5(6) (2015) 4675-4680.

[16] J. Garcia-Amorós, M. Reig, A. Cuadrado, M. Ortega, S. Nonell, D. Velasco, A photoswitchable bis-azo derivative with a high temporal resolution, Chemical Communications 50(78) (2014) 11462-11464.

[17] A.A. Zaki, H. Ahmed, M. Hagar, Impact of fluorine orientation on the optical properties of difluorophenylazophenyl benzoates liquid crystal, Materials Chemistry and Physics 216 (2018) 316-324.

[18] M.H. H. A. Ahmed, T. H. El-Sayed and R. Alnoman Schiff Base/Ester Liquid Crystals with Different Lateral Substituents: Mesophase Behaviour and DFT Calculations, Liquid crystals in press.

[19] M.M. Naoum, N.H. Metwally, M.M. Abd Eltawab, H.A. Ahmed, Polarity and steric effect of the lateral substituent on the mesophase behaviour of some newly prepared liquid crystals, Liquid Crystals 42(10) (2015) 1351-1369.

[20] H. Ahmed, G. Saad, Mesophase behaviour of laterally di-fluoro-substituted four-ring compounds, Liquid Crystals 42(12) (2015) 1765-1772.

[21] M. Naoum, A. Fahmi, H. Ahmed, Effect of the relative orientation of the two fluoro-substituents on the mesophase behavior of phenylazophenyl benzoates, Molecular Crystals and Liquid Crystals 562(1) (2012) 43-65.

[22] M. Naoum, A. Fahmi, H. Ahmed, Liquid crystalline behaviour of model compounds di-laterally substituted with different polar groups, Liquid Crystals 38(4) (2011) 511-519.

[23] M. Naoum, H. Ahmed, Effect of dipole moment and conformation on the mesophase behavior of di-laterally substituted phenylazophenyl benzoate liquid crystals, Thermochimica acta 521(1-2) (2011) 202-210.

[24] M. Naoum, S. Mohammady, H. Ahmed, Lateral protrusion and mesophase behaviour in pure and mixed states of model compounds of the type 4-(4′-substituted phenylazo)-2-(or 3-) methyl phenyl-4'-alkoxy benzoates, Liquid Crystals 37(10) (2010) 1245-1257.

[25] W. Zhou, H. Yu, Different morphologies of self-assembled nanofibers fabricated with amphiphilic low-molecular-weight azopyridinium salts, RSC Advances 3(44) (2013) 22155-22159.

[26] W. Zhou, T. Kobayashi, H. Zhu, H. Yu, Electrically conductive hybrid nanofibers constructed with two amphiphilic salt components, Chemical Communications 47(48) (2011) 12768-12770.

[27] H. Zhang, R. Hao, J.K. Jackson, M. Chiao, H. Yu, Janus ultrathin film from multi-level self-assembly at air–water interfaces, Chemical Communications 50(94) (2014) 14843-14846.

[28] J.-i. Mamiya, A. Yoshitake, M. Kondo, Y. Yu, T. Ikeda, Is chemical crosslinking necessary for the photoinduced bending of polymer films?, Journal of Materials Chemistry 18(1) (2008) 63-65.

[29] K.i. Aoki, M. Nakagawa, K. Ichimura, Self-assembly of amphoteric azopyridine carboxylic acids: organized structures and macroscopic organized morphology influenced by heat, pH change, and light, Journal of the American Chemical Society 122(44) (2000) 10997-11004.

[30] M. Alaasar, C. Tschierske, M. Prehm, Hydrogen-bonded supramolecular complexes formed between isophthalic acid and pyridine-based derivatives, Liquid Crystals 38(7) (2011) 925-934.

[31] H. Ahmed, M. Naoum, Mesophase behaviour of azobenzene-based angular supramolecular hydrogen-bonded liquid crystals, Liquid Crystals 43(2) (2016) 222-234.

[32] M.M. Naoum, A.A. Fahmi, A.A. Refaie, M.A. Alaasar, Novel hydrogen-bonded angular supramolecular liquid crystals, Liquid Crystals 39(1) (2012) 47-61.

[33] M. Naoum, A. Fahmi, M. Alaasar, Supramolecular hydrogen-bonded liquid crystals formed from 4-(4′-pyridylazophenyl)-4 ″-alkoxy benzoates and 4-substituted benzoic acids, Molecular Crystals and Liquid Crystals 487(1) (2008) 74-91.

[34] M. Naoum, A. Fahmi, M. Alaasar, Supramolecular liquid crystals induced by hydrogen-bonding interactions between non-mesomorphic compounds. I. 4-(4′-Pyridylazophenyl)-4 ″-substituted benzoates and 4-substituted benzoic acids, Molecular Crystals and Liquid Crystals 506(1) (2009) 22-33.

[35] M.M. Naoum, A.G.A. Fahmi, W.A. Almllal, Supramolecular Liquid Crystals Induced by Hydrogen-Bonding Interactions between Non-Mesomorphic Compounds. II. Effect of Lateral Substitution, Molecular Crystals and Liquid Crystals 518(1) (2010) 109-128.

[36] H. Ahmed, M. Hagar, O. Alhaddad, New chair shaped supramolecular complexes-based aryl nicotinate derivative; mesomorphic properties and DFT molecular geometry, RSC Advances 9(29) (2019) 16366-16374.

[37] K.-y. Chen, Crystal Structure, Hydrogen-Bonding Properties, and DFT Studies of 2-((2-(2-Hydroxyphenyl) benzo [d] thiazol-6-yl) methylene) malononitrile, Molecular Crystals and Liquid Crystals 623(1) (2015) 285-296.

[38] M. Shoji, F. Tanaka, Theoretical study of hydrogen-bonded supramolecular liquid crystals, Macromolecules 35(19) (2002) 7460-7472.

[39] S. Sundaram, R. Jayaprakasam, M. Dhandapani, T. Senthil, V. Vijayakumar, Theoretical (DFT) and experimental studies on multiple hydrogen bonded liquid crystals comprising between aliphatic and aromatic acids, Journal of Molecular Liquids 243 (2017) 14-21.

[40] M. Hagar, H. Ahmed, O. Alhaddadd, DFT Calculations and Mesophase Study of Coumarin Esters and Its Azoesters, Crystals 8(9) (2018) 359.

[41] M. Hagar, S.M. Soliman, F. Ibid, H. El Sayed, Quinazolin-4-yl-sulfanylacetyl-hydrazone derivatives; Synthesis, molecular structure and electronic properties, Journal of Molecular Structure 1049 (2013) 177-188.

[42] S.M. Soliman, M. Hagar, F. Ibid, H. El Sayed, Experimental and theoretical spectroscopic studies, HOMO–LUMO, NBO analyses and thione–thiol tautomerism of a new hybrid of 1, 3, 4-oxadiazole-thione with quinazolin-4-one, Spectrochimica Acta Part A: Molecular and Biomolecular Spectroscopy 145 (2015) 270-279.

[43] M. Hagar, S.M. Soliman, F. Ibid, H. El Sayed, Synthesis, molecular structure and spectroscopic studies of some new quinazolin-4 (3H)-one derivatives; an account on the N-versus S-Alkylation, Journal of Molecular Structure 1108 (2016) 667-679.

[44] A. Aboelnaga, M. Hagar, S.M. Soliman, Ultrasonic Synthesis, Molecular Structure and Mechanistic Study of 1, 3-Dipolar Cycloaddition Reaction of 1-Alkynylpyridinium-3-olate and Acetylene Derivatives, Molecules 21(7) (2016) 848.

[45] D.A. Paterson, M. Gao, Y.-K. Kim, A. Jamali, K.L. Finley, B. Robles-Hernández, S. Diez-Berart, J. Salud, M.R. de la Fuente, B.A. Timimi, Understanding the twist-bend nematic phase: the characterisation of 1-(4-cyanobiphenyl-4′-yloxy)-6-(4-cyanobiphenyl-4′-yl) hexane (CB6OCB) and comparison with CB7CB, Soft Matter 12(32) (2016) 6827-6840.

[46] A. Martinez-Felipe, A.G. Cook, J.P. Abberley, R. Walker, J.M. Storey, C.T. Imrie, An FT-IR spectroscopic study of the role of hydrogen bonding in the formation of liquid crystallinity for mixtures containing bipyridines and 4-pentoxybenzoic acid, RSC Advances 6(110) (2016) 108164-108179.

[47] M. Hagar, H. Ahmed, G. Saad, Synthesis and mesophase behaviour of Schiff base/ester 4-(arylideneamino) phenyl-4 ″-alkoxy benzoates and their binary mixtures, Journal of Molecular Liquids 273 (2019) 266-273.

[48] R. Chen, Z. An, W. Wang, X. Chen, P. Chen, Lateral substituent effects on UV stability of high-birefringence liquid crystals with the diaryl-diacetylene core: DFT/TD-DFT study, Liquid Crystals 44(10) (2017) 1515-1524.

[49] M. Hagar, H. Ahmed, O. Alhaddad, Experimental and theoretical approaches of molecular geometry and mesophase behaviour relationship of laterally substituted azopyridines, Liquid Crystals (2019) 1-12.

[50] H.K. Cammenga, W. Eysel, E. Gmelin, W. Hemminger, G.W. Höhne, S.M. Sarge, The temperature calibration of scanning calorimeters: Part 2. Calibration substances, Thermochimica Acta 219 (1993) 333-342.

[51] M. Frisch, G. Trucks, H.B. Schlegel, G. Scuseria, M. Robb, J. Cheeseman, G. Scalmani, V. Barone, B. Mennucci, G. Petersson, Gaussian 09, revision a. 02, gaussian, Inc., Wallingford, CT 200 (2009).

[52] R. Dennington, T. Keith, J. Millam, GaussView, version 5, (2009).

[53] H.A. Ahmed, M. Hagar, O.A. Alhaddad, Phase behavior and DFT calculations of laterally methyl supramolecular hydrogen-bonding complexes, Crystals 9(3) (2019) 133.

[54] H. Ahmed, M. Hagar, A. Aljuhani, Mesophase behavior of new linear supramolecular hydrogen-bonding complexes, RSC Advances 8(61) (2018) 34937-34946.

[55] W. Cleland, M.M. Kreevoy, Low-barrier hydrogen bonds and enzymic catalysis, Science 264(5167) (1994) 1887-1890.

[56] M. Lizu, M. Lutfor, N. Surugau, S. How, S.E. Arshad, Synthesis and characterization of ethyl cellulose–based liquid crystals containing azobenzene chromophores, Molecular Crystals and Liquid Crystals 528(1) (2010) 64-73.

[57] A. Martínez-Felipe, C.T. Imrie, The role of hydrogen bonding in the phase behaviour of supramolecular liquid crystal dimers, Journal of Molecular Structure 1100 (2015) 429-437.

[58] A. Ghanem, C. Noel, FTIR investigation of two alkyl-p-terphenyl-4, 4 ″-dicarboxylates in their crystalline, smectic and isotropic phases, Molecular Crystals and Liquid Crystals 150(1) (1987) 447-472.

[59] D.A. Paterson, A. Martínez-Felipe, S.M. Jansze, A. TM Marcelis, J. MD Storey, C.T. Imrie, New insights into the liquid crystal behaviour of hydrogen-bonded mixtures provided by temperature-dependent FTIR spectroscopy, Liquid Crystals 42(5-6) (2015) 928-939.

[60] R. Walker, D. Pociecha, J. Abberley, A. Martinez-Felipe, D. Paterson, E. Forsyth, G. Lawrence, P. Henderson, J. Storey, E. Gorecka, Spontaneous chirality through mixing achiral components: a twist-bend nematic phase driven by hydrogen-bonding between unlike components, Chemical Communications 54(27) (2018) 3383-3386.

[61] H. Ahmed, M. Naoum, G. Saad, Mesophase behaviour of 1: 1 mixtures of 4-n-alkoxyphenylazo benzoic acids bearing terminal alkoxy groups of different chain lengths, Liquid Crystals 43(9) (2016) 1259-1267.

[62] B. Thaker, J. Kanojiya, R. Tandel, Effects of different terminal substituents on the mesomorphic behavior of some azo-schiff base and azo-ester-based liquid crystals, Molecular Crystals and Liquid Crystals 528(1) (2010) 120-137.

[63] M.M. Naoum, A.A. Fahmi, M.A. Alaasar, R.A. Salem, Supramolecular liquid crystals in binary and ternary systems, Thermochimica acta 517(1-2) (2011) 63-73.

[64] H. Ahmed, M. Hagar, T. El-Sayed, R. B. Alnoman, Schiff base/ester liquid crystals with different lateral substituents: mesophase behaviour and DFT calculations, Liquid Crystals (2019) 1-11.

[65] H. Ahmed, M. Hagar, G. Saad, Impact of the proportionation of dialkoxy chain length on the mesophase behaviour of Schiff base/ester liquid crystals; experimental and theoretical study, Liquid Crystals (2019) 1-10.

[66] M. Hagar, H. Ahmed, O. Alhaddad, New azobenzene-based natural fatty acid liquid crystals with low melting point: synthesis, DFT calculations and binary mixtures, Liquid Crystals (2019) 1-12.

[67] C. Imrie, Laterally substituted dimeric liquid crystals, Liquid Crystals 6(4) (1989) 391-396.

[68] J. Schroeder, D. Bristol, Liquid crystals. IV. Effects of terminal substituents on the nematic mesomorphism of p-phenylene dibenzoates, The Journal of Organic Chemistry 38(18) (1973) 3160-3164.